Observational evidence for a negative shortwave cloud feedback in mid to high latitudes

Paulo Ceppi,[1,2] Daniel T. McCoy,[1] and Dennis L. Hartmann[1]

Corresponding author: P. Ceppi, Department of Meteorology, University of Reading, Earley Gate, PO Box 243, RG6 6BB, Reading, United Kingdom. (p.ceppi@reading.ac.uk)

[1]Department of Atmospheric Sciences,
University of Washington, Seattle, WA,
USA.

[2]Department of Meteorology, University
of Reading, Reading, United Kingdom.

Key Points.

- A negative shortwave cloud feedback is observed in mid to high Southern latitudes.
- This negative feedback results from increasing cloud optical depth with temperature.
- Models are in qualitative agreement with observations in mid to high latitudes.

Abstract.

Exploiting the observed robust relationships between temperature and optical depth in extratropical clouds, we calculate the shortwave cloud feedback from historical data, by regressing observed and modeled cloud property histograms onto local temperature in mid to high Southern latitudes. In this region, all CMIP5 models and observational data sets predict a negative cloud feedback, mainly driven by optical thickening. Between 45° and 60° S, the mean observed shortwave feedback (-0.91 ± 0.82 W m^{-2} K^{-1}, relative to local rather than global-mean warming) is very close to the multi-model mean feedback in RCP8.5 (-0.98 W m^{-2} K^{-1}), despite differences in the meridional structure. In models, historical temperature–cloud property relationships reliably predict the forced RCP8.5 response. Because simple theory predicts this optical thickening with warming, and cloud amount changes are relatively small, we conclude that the shortwave cloud feedback is very likely negative in the real world at mid to high latitudes.

1. Introduction

The cloud feedback has been identified as the dominant source of uncertainty in model-based estimates of climate sensitivity, primarily because of the shortwave radiation response associated with tropical low clouds [*Boucher et al.*, 2013]. To a large extent, the uncertain cloud-radiative response reflects difficulties in representing the effects of small-scale processes on the cloud water budget in coarse climate model grids using parameterizations. Among the most uncertain parameterized processes are those related to convective mixing [*Zhao*, 2014; *Sherwood et al.*, 2014; *Webb et al.*, 2015] as well as ice-phase cloud microphysics [*Storelvmo et al.*, 2015, and references therein].

Despite these large uncertainties persisting across generations of climate models, some robust signals emerge. In terms of the shortwave (SW) cloud feedback, current models agree on a negative feedback in mid to high latitudes, mainly caused by an optical thickening and brightening of the clouds [*Zelinka et al.*, 2012a; *Gordon and Klein*, 2014; *Ceppi et al.*, 2016]. Warming-induced phase changes in mixed-phase clouds (dominant in mid to high latitudes) are believed to be an important driver of this optical thickening, at least in models [*Tsushima et al.*, 2006; *McCoy et al.*, 2014; *Ceppi et al.*, 2016], although increases in the "adiabatic" cloud water content could also contribute [*Somerville and Remer*, 1984; *Betts and Harshvardhan*, 1987; *Tselioudis et al.*, 1992]. In models, the relationship between optical depth and temperature remains similar across timescales, so that the forced optical depth response in global warming experiments is well-predicted by unforced seasonal or interannual fluctuations [*Gordon and Klein*, 2014]. This supports the idea that the cloud optical depth increase in high latitudes is a direct response to

warming, and suggests that the associated negative SW feedback might be predictable from historical data. To our knowledge, however, the robust optical depth–temperature relationships have not been exploited thus far to predict the SW cloud feedback in models and observations.

The purpose of this paper is to demonstrate that the cloud water increase, and the associated optical thickening and negative SW feedback in mid to high latitudes, can all be detected from historical data in both models and observations in the Southern Hemisphere. Furthermore, the SW cloud feedback in the RCP8.5 experiment is well-predicted from historical model simulations in mixed-phase regions, consistent with the time scale-invariance of optical depth–temperature relationships found in previous studies. While observational uncertainties and disagreements between satellite products limit our ability to produce accurate quantitative estimates of the SW cloud feedback in the real world, we will show that models and observations are in qualitative agreement on this negative SW cloud feedback.

2. Data and Methods

This study combines observed and modeled cloud property data, all in monthly-mean resolution. We first briefly describe the satellite observations. Liquid water path changes are assessed using 20 years of satellite microwave retrievals [UWisc data set; *O'Dell et al.*, 2008], covering the period January 1989 to December 2008. Additionally, we use cloud amount retrievals, available from three satellite-based data sets: ISCCP [*Rossow and Schiffer*, 1999], MISR [*Diner et al.*, 1998] and MODIS [*King et al.*, 2003; *Platnick et al.*, 2003], providing 25, 12, and 14 years of data, respectively. These cloud amount retrievals have been binned into cloud top pressure (or height) versus optical depth histograms.

For details on the preparation of these simulator-oriented data sets, see *Marchand et al.* [2010], *Zhang et al.* [2012], *Pincus et al.* [2012], and *Marchand* [2013], as well as Text S1.

The model data used here include output from the historical and RCP8.5 experiments, where the RCP8.5 response or feedback is based on differences between 1981–2000 and 2081–2100. The 30 models included in this study are listed in the Supporting Information, Table S1. Only a subset of these models provide cloud property histograms for comparison with observations, and due to limited availability of historical cloud histogram data we also use AMIP output (see Table S1). These cloud histograms are produced using satellite simulators, which mimic the cloud properties that would be retrieved by a satellite if the modeled clouds existed in the real world; for details, see *Klein and Jakob* [1999], *Webb et al.* [2001], and *Klein et al.* [2013]. We have verified correct simulator implementation in these models as in *Zelinka et al.* [2012b] (see Text S1 for details).

As outlined in the Introduction, the main goal of this study is to demonstrate the existence of a negative cloud optical depth feedback in mid to high latitudes that is detectable in the context of unforced seasonal or interannual variability. Assuming this feedback is mainly driven by the direct effect of local warming, we estimate the SW cloud feedback in two steps. In the first step, we regress cloud property histograms onto local lower-tropospheric temperature (defined as the 500–850 hPa layer mean) in models and observations. The choice of this pressure range is based on the fact that the bulk of cloud water is typically contained in this layer in models [see e.g. *Komurcu et al.*, 2014; *Ceppi et al.*, 2016]. For models, we use 1981–2000 historical or AMIP data; for observations, the satellite data are regressed onto ERA-Interim reanalysis temperature using the full length of each of the satellite products. The regressions are calculated at each latitude, using

data for all months and longitudes linearly interpolated onto the cloud histogram grid. Prior to the regression analysis, we remove the annual-mean value at every gridpoint, and average the data over non-overlapping, 20°-wide longitude boxes. This last step ensures that the cloud anomalies are nearly uncorrelated between adjacent longitude points, and can be treated as independent realizations in both time and longitude space, which is necessary for an accurate estimation of confidence intervals for the regression slopes.

Note that since some of the satellite instruments do not report values over land or sea ice gridpoints, only ocean gridpoints are included in the regression analysis, and we restrict the analysis to the Southern Hemisphere where most midlatitude areas are ocean-covered. Furthermore, because instruments measuring solar reflectance (such as ISCCP, MISR, and MODIS) are known to produce large positive biases in cloud optical depth at high solar zenith angles [*Loeb and Davies*, 1996], for MISR and MODIS we exclude points with solar zenith angle $> 60°$ at the time of satellite overpass. For ISCCP, the results exhibit very little sensitivity to the exclusion of high solar zenith angle retrievals (not shown), so such retrievals are included in the analysis. The sensitivity of the results to these choices is discussed in the Supporting Information.

In the second step, the cloud property histogram regressions are converted to anomalous top-of-atmosphere SW radiative fluxes by multiplying with SW cloud-radiative kernels [described in *Zelinka et al.*, 2012b] and integrating over all 49 (7×7) cloud top pressure–optical depth bins. This yields a cloud feedback in units of W m^{-2} K^{-1}, which we call the "predicted" cloud feedback, and we compare it with the "actual" feedback in RCP8.5 obtained by the approximate partial radiative perturbation method [APRP; *Taylor et al.*, 2007]. Since the cloud-radiative kernels are functions of surface albedo, we use a 15-year

climatology (March 2000–February 2015) of CERES EBAF clear-sky surface upward and downward SW fluxes [*Loeb et al.*, 2009] to calculate the observed surface albedo. Also, because we assume that the cloud property–temperature relationships are independent of the month of the year, the cloud-radiative kernels are averaged over all calendar months prior to multiplication with the cloud histogram regression matrices.

3. Results

3.1. Observed and modeled changes in LWP and cloud amount

We begin by assessing how temperature affects two key cloud properties relevant to SW radiation, cloud liquid water path (LWP) and cloud amount (or fractional coverage), in the mid to high Southern latitudes. Models and observations agree on a positive relationship between LWP and low-level temperature (Fig. 1a), although the magnitude of the relationship varies considerably among models. Compared to most models, the observed LWP–temperature relationship is weaker in magnitude poleward of about 47° S and stronger equatorward thereof, but is very highly statistically significant, and remains the same whether the seasonal cycle is removed or not (thin and thick red curves in Fig. 1a). Because cloud optical thickness is approximately linearly proportional to the LWP [*Stephens*, 1978], the positive LWP–temperature relationships imply optical thickening with warming. Assuming these relationships hold for the forced global warming case, and all other things remaining equal, one would thus expect brighter clouds and therefore a negative SW cloud feedback to occur in mid to high latitudes.

Note that although Fig. 1a–b shows gridbox-mean rather than in-cloud LWP values, the LWP increases are *not* due to cloud amount increases; the results remain qualitatively unchanged if the LWP values are normalized by cloud fraction before calculating the

response (not shown). Furthermore, the cloud amount and LWP changes are essentially uncorrelated across models over the 45°–60° S region ($r = 0.06$). While cloud reflectivity is also affected by changes in ice water path (IWP, not shown here), the cloud ice response is substantially smaller than the LWP change in RCP8.5 [see Fig. 1 in *Ceppi et al.*, 2016], suggesting this is a second-order effect in models.

Another potential effect of clouds on SW radiation comes from cloud amount changes. While the cloud amount sensitivity to low-level temperature is very model-dependent, the mean model behavior is to increase cloud cover poleward of about 50° S with warming, with a weak decrease equatorward thereof (Fig. 1c). By contrast, all three satellite instruments show a weak but statistically significant cloud amount increase with warming at all latitudes poleward of about 40° S. Although they agree on the sign of the response, quantitative differences exist, with MODIS systematically indicating the largest cloud fraction increases. It should be noted that in observations, low-level temperature is highly correlated with lower-tropospheric stability [as measured by the estimated inversion strength; *Wood and Bretherton*, 2006] over the Southern midlatitudes (not shown). Since low-level stability is an important control on low cloud amount [*Klein and Hartmann*, 1993; *Wood and Bretherton*, 2006], the observed positive cloud amount–temperature relationship may in fact reflect the effect of boundary-layer stability on low cloud amount, rather than a direct effect of temperature. The influence of low-level stability on low cloud amount appears to be underestimated by models [*Qu et al.*, 2015].

The historical relationships between cloud properties and temperature are useful indicators of the cloud feedback only to the extent that they accurately predict future changes. So, are the predicted and actual cloud responses similar? The bottom row of Fig. 1 shows

the actual LWP and cloud amount response in the RCP8.5 experiment, for comparison with the predicted response. Note that although the RCP8.5 response is not purely temperature-driven and also contains a direct CO_2 effect [*Sherwood et al.*, 2015], the cloud response in AMIP4K is very similar (not shown), suggesting that the response is mainly warming-induced. Overall, the actual responses are remarkably similar to those predicted from historical model data in an ensemble-mean sense. Comparing the responses across models, we find that the predicted and actual LWP changes are well-correlated over the 45°–60° S latitude range and close to the one-to-one line (Fig. 2a), suggesting that future LWP changes are reasonably well-predicted by historical relationships. In this and following scatterplots, we use the uncertainty in the relationship between predicted and actual response in models to derive observational confidence intervals, such that the confidence interval width is proportional to the standard deviation of the residuals relative to the one-to-one line (Text S3).

The relationship between actual and predicted cloud amount change is also positive, but the agreement is weaker than for LWP (Fig. 2b). However, we will show that increasing optical depth, rather than cloud amount, is the main driver of the negative SW cloud feedback simulated by models in mid to high latitudes. The scatterplots in Fig. 2 demonstrate that historical, seasonal relationships between cloud properties and local temperature are representative of the forced, long-term cloud response to future warming. They also illustrate that in the 45°–60° S region, models generally overestimate the LWP increase compared to observations (vertical red bar in Fig. 2a), in some cases by a considerable amount. By contrast, the predicted cloud amount change tends to be

less positive than in observations, although the difference is small. The implications of these differences on the SW cloud feedback will be discussed in the next subsection.

3.2. Observed and modeled SW cloud feedback

To estimate the SW cloud feedback in models and observations, under the assumption the feedback is mainly driven by local temperature changes, we proceed as in the previous section and regress the cloud amount histograms onto low-level temperature. Given the robust increases in LWP seen in the mid to high Southern latitudes, we expect to find a shift in the cloud amount histogram toward higher optical depth as temperature increases. As illustrated in Fig. 3, this is indeed the case: over the 45°–60° S region, the cloud amount response mainly consists of a dipole along the optical depth dimension, reflecting a shift of the climatological cloud distribution toward higher τ values. The cloud histogram responses in MISR (Fig. S1), MODIS (Fig. S2), and the model ISCCP simulators (not shown) are all qualitatively similar. The cloud histogram regression matrices (illustrated in Fig. 3b) are multiplied with the SW cloud-radiative kernel at each latitude to yield a predicted SW cloud feedback (see Methods).

As expected from the results above, models and observations predict a negative SW cloud feedback poleward of about 45° S, coincident with the region of increasing LWP with temperature (Fig. 4a). While different observational data sets disagree on the magnitude of the negative feedback, especially at the highest latitudes, they agree on the sign and overall latitudinal structure. They are also consistent with the bulk of the model distribution, although the observed negative feedback pattern appears to be shifted toward lower latitudes compared with most models. This shift agrees qualitatively with the differences in the LWP and cloud amount responses to warming (cf. Fig. 1a–b). The predicted

cloud feedback is remarkably similar to the actual RCP8.5 cloud feedback in this set of climate models both in terms of magnitude and meridional structure (Fig. 4b), and the values are well-correlated across models in the 45°–60° S latitude band (Fig. 5), confirming the idea that historical temperature–cloud brightness relationships are representative of long-term changes [*Gordon and Klein*, 2014].

Averaging the three observational estimates together, we find a mean observed SW feedback of -0.91 ± 0.82 W m^{-2} K^{-1}, significantly negative, and close to the mean actual feedback in RCP8.5 (-0.98 W m^{-2} K^{-1}). It should be noted, however, that the close agreement between observations and models in Fig. 5 masks disagreements in the meridional structure of the cloud feedback, as described in the previous paragraph. Such disagreements in the meridional structure of the SW cloud feedback may have important implications for the models' ability to correctly simulate the spatial distribution of the temperature response.

Using the cloud property histograms allows us to decompose the cloud feedback into effects of cloud optical depth and cloud amount changes (Fig. S3), following the method of *Zelinka et al.* [2013]. In general, the optical depth increase explains most of the negative SW cloud feedback in observations and for the multi-model mean, although cloud amount changes do contribute substantially to the inter-model spread in SW feedback. For MODIS, the optical depth and cloud amount effects appear to be of comparable magnitude poleward of 45° S, while the other two satellite data sets predict a larger (more negative) optical depth feedback. Hence, Fig. S3 shows that the disagreement in the magnitude of the observed negative cloud feedback in Southern midlatitudes between satellite products is mainly associated with the optical depth effect rather than with cloud

amount changes. Note that there are two additional terms in this decomposition of the cloud histogram response, one reflecting the effect of cloud altitude changes and another representing a residual term [see *Zelinka et al.*, 2013]; both are very small (not shown).

4. Discussion

The results in the previous section have shown that in mid to high Southern latitudes,

1. cloud optical depth increases with warming are detectable in observations and historical model simulations,

2. in models the historical seasonal optical depth–temperature relationships are good predictors of the future SW cloud feedback, and

3. the predicted negative SW cloud feedback is qualitatively similar in models and observations.

The ubiquity of this negative feedback across models and observations is likely at least in part a result of robust phase changes in mixed-phase cloud regions, which cause increases in LWP and optical depth with warming [*Tsushima et al.*, 2006; *McCoy et al.*, 2014; *Storelvmo et al.*, 2015; *Ceppi et al.*, 2016]. While the possible importance of the phase change effect in the real world is difficult to demonstrate due to limitations in the availability and quality of cloud phase observations, changes in microphysical phase conversion rates have been shown to be the main driver of the negative optical depth feedback in models [*Ceppi et al.*, 2016]. Differences in the parameterization of microphysical phase change processes also likely account for at least part of the large inter-model differences in LWP and cloud optical depth sensitivity to warming [*Komurcu et al.*, 2014; *McCoy et al.*, 2015; *Cesana et al.*, 2015].

Although the three satellite data sets are in qualitative agreement on an optical thickening (and associated negative SW cloud feedback) in high Southern latitudes, and are in relatively close agreement in a regional mean sense (the 45°–60° S–mean feedback ranging between -0.76 W m^{-2} K^{-1} for MODIS and -1.07 W m^{-2} K^{-1} for MISR), the differences between data sets are not negligible locally (cf. Figs. 4 and S3), reflecting disagreements in the cloud optical depth response to warming (Fig. S4). We believe the differences between observational data sets result from relatively large uncertainties in the satellite retrievals of cloud properties, with the uncertainty sources being specific to each data set. Some known error sources, and their possible impacts on our results, are discussed in the Supporting Information (Text S2). It should be kept in mind that measurement errors due to illumination and viewing angle, for example, are not included in the instrument simulators in climate models. For this reason, instrument simulators may better reflect the clouds in the models than real satellite observations characterize clouds in nature.

In addition to the uncertainty associated with errors in satellite retrievals, further uncertainty in the magnitude of the real SW cloud feedback results from the imperfect prediction of future responses from historical model data, as illustrated in the scatterplots in Figs. 2 and 5; the calculation of the observational confidence intervals is derived from this uncertainty (Text S3). The differences between predicted and actual response result from effects not accounted for by the simple regression on local temperature; an obvious example would be the radiative effect of increasing CO_2 concentrations, but other factors such as atmospheric circulation, lower-tropospheric stability, vertical and horizontal moisture fluxes, to name a few, are likely also contributing to the forced cloud response.

Despite the current shortcomings of cloud property observations, we believe that the positive optical depth–temperature relationships are real and physical for the following two reasons: (a) four independent observational data sets and all CMIP5 models agree on mixed-phase clouds becoming optically thicker (or equivalently, their water content increasing) with warming, and (b) in such cold clouds a positive optical depth–temperature relationship is *expected* from relatively basic physical temperature-related mechanisms (phase transitions, and increasing adiabatic water content). (Note that while optical depth increases linearly with LWP only assuming constant droplet radius [*Stephens*, 1978], a more realistic assumption of constant particle number also leads to higher optical depth as LWP increases.) With no indication of compensating large cloud amount decreases with warming in the real world, and strong observational and modeling evidence for optical depth increases, we conclude that the shortwave cloud feedback in a future warmer climate will very likely be negative in mid to high Southern latitudes.

5. Conclusions

Using historical CMIP5 model data and satellite retrievals of cloud properties, we have shown that as the atmosphere warms, cloud liquid water (and hence optical depth) consistently increase in mid to high latitudes (poleward of $\sim 45°$) in the Southern Hemisphere, with an additional weak cloud amount response to warming. Although models disagree on the magnitude of the cloud liquid water increase, it is present in all models and in observations, and is supported by robust temperature-dependent mechanisms (phase changes in mixed-phase clouds, and adiabatic cloud water content increases). To estimate the SW radiation response associated with the optical thickening of the clouds, cloud property histograms binned by cloud top pressure and optical depth are regressed

on lower-tropospheric temperature and combined with cloud-radiative kernels [*Zelinka et al.*, 2012b]. Consistent with the cloud water response, all models and observational data sets predict a negative SW cloud feedback in mid to high Southern latitudes, and observations lie well within the model distribution. In the 45°–60° S latitude band, the predicted feedback in observations ranges between -0.76 W m^{-2} K^{-1} (MODIS) and -1.07 W m^{-2} K^{-1} (MISR), with an estimated mean value of -0.91 ± 0.82 W m^{-2} K^{-1}, close to the actual feedback in RCP8.5 (-0.98 W m^{-2} K^{-1}). For models, the feedback predicted from historical seasonal temperature variations is a good predictor of the actual feedback in the RCP8.5 experiment ($r = 0.78$), supporting the idea that a warming-induced cloud optical depth increase is detectable in the historical record.

Observed cloud optical depth–temperature relationships in extratropical clouds have been proposed as a promising potential observational constraint on modeled cloud feedbacks by *Klein and Hall* [2015], who also note that such observational constraints must be supported by a robust, well-understood physical mechanism in order to be credible. In the context of the cloud optical depth feedback, an important question for future work is therefore to clarify the relative importance of phase change effects and adiabatic water content increases in observations and models. This highlights the need for reliable cloud property observations — particularly cloud phase — in sufficient spatial and temporal coverage.

Acknowledgments. We thank Robert Pincus, Chris Terai, Mark Zelinka, and two reviewers for very useful comments on the manuscript, as well as Roger Marchand, Chris Bretherton, and Rob Wood for helpful discussions. We are also very grateful to Mark Zelinka for developing and providing the cloud-radiative kernels (`http://www.atmos.`

washington.edu/~mzelinka/kernels/). We acknowledge the World Climate Research Program's Working Group on Coupled Modeling, which is responsible for CMIP, and we thank the climate modeling groups (listed in Table S1 of this paper) for producing and making available their model output. For CMIP the U.S. Department of Energy's Program for Climate Model Diagnosis and Intercomparison provides coordinating support and led development of software infrastructure in partnership with the Global Organization for Earth System Science Portals. The data used are described in section 2 and in the Supporting Information, Text S1 and Table S1. This work was supported by the National Science Foundation under grant AGS-0960497.

References

Betts, A. K., and Harshvardhan (1987), Thermodynamic constraint on the cloud liquid water feedback in climate models, *Journal of Geophysical Research*, *92*(D7), 8483, doi: 10.1029/JD092iD07p08483.

Boucher, O., D. Randall, P. Artaxo, C. Bretherton, G. Feingold, P. Forster, V.-M. Kerminen, Y. Kondo, H. Liao, U. Lohmann, P. Rasch, S. K. Satheesh, S. Sherwood, B. Stevens, and X. Y. Zhang (2013), Clouds and Aerosols, in *Climate Change 2013: The Physical Science Basis. Contribution of Working Group I to the Fifth Assessment Report of the Intergovernmental Panel on Climate Change*, edited by T. F. Stocker, D. Qin, P. G.-K, M. Tignor, S. K. Allen, J. Boschung, A. Nauels, Y. Xia, V. Bex, and P. M. Midgley, pp. 571–657, Cambridge University Press, Cambridge, United Kingdom and New York, NY, USA, doi:10.1017/CBO9781107415324.

Ceppi, P., D. L. Hartmann, and M. J. Webb (2016), Mechanisms of the negative shortwave cloud feedback in high latitudes, *Journal of Climate*, *29*(1), 139–157, doi: 10.1175/JCLI-D-15-0327.1.

Cesana, G., D. E. Waliser, X. Jiang, and J.-L. F. Li (2015), Multi-model evaluation of cloud phase transition using satellite and reanalysis data, *Journal of Geophysical Research: Atmospheres*, *120*, doi:10.1002/2014JD022932.

Diner, D., J. Beckert, T. Reilly, C. Bruegge, J. Conel, R. Kahn, J. Martonchik, T. Ackerman, R. Davies, S. Gerstl, H. Gordon, J. Muller, R. Myneni, P. Sellers, B. Pinty, and M. Verstraete (1998), Multi-angle Imaging SpectroRadiometer (MISR) instrument description and experiment overview, *IEEE Transactions on Geoscience and Remote Sensing*, *36*(4), 1072–1087, doi:10.1109/36.700992.

Gordon, N. D., and S. A. Klein (2014), Low-cloud optical depth feedback in climate models, *Journal of Geophysical Research: Atmospheres*, *119*(10), 6052–6065, doi:10.1002/2013JD021052.

King, M., W. Menzel, Y. Kaufman, D. Tanre, S. Platnick, S. Ackerman, L. Remer, R. Pincus, and P. Hubanks (2003), Cloud and aerosol properties, precipitable water, and profiles of temperature and water vapor from MODIS, *IEEE Transactions on Geoscience and Remote Sensing*, *41*(2), 442–458, doi:10.1109/TGRS.2002.808226.

Klein, S. A., and A. Hall (2015), Emergent Constraints for Cloud Feedbacks, *Current Climate Change Reports*, *1*(4), 276–287, doi:10.1007/s40641-015-0027-1.

Klein, S. A., and D. L. Hartmann (1993), The Seasonal Cycle of Low Stratiform Clouds, *Journal of Climate*, *6*(8), 1587–1606, doi:10.1175/1520-0442(1993)006⟨1587:TSCOLS⟩2.0.CO;2.

Klein, S. A., and C. Jakob (1999), Validation and Sensitivities of Frontal Clouds Simulated by the ECMWF Model, *Monthly Weather Review*, *127*(10), 2514–2531, doi:10.1175/1520-0493(1999)127⟨2514:VASOFC⟩2.0.CO;2.

Klein, S. A., Y. Zhang, M. D. Zelinka, R. Pincus, J. Boyle, and P. J. Gleckler (2013), Are climate model simulations of clouds improving? An evaluation using the ISCCP simulator, *Journal of Geophysical Research: Atmospheres*, *118*(3), 1329–1342, doi:10.1002/jgrd.50141.

Komurcu, M., T. Storelvmo, I. Tan, U. Lohmann, Y. Yun, J. E. Penner, Y. Wang, X. Liu, and T. Takemura (2014), Intercomparison of the cloud water phase among global climate models, *Journal of Geophysical Research: Atmospheres*, *119*(6), 3372–3400, doi:10.1002/2013JD021119.

Loeb, N. G., and R. Davies (1996), Observational evidence of plane parallel model biases: Apparent dependence of cloud optical depth on solar zenith angle, *Journal of Geophysical Research*, *101*(D1), 1621, doi:10.1029/95JD03298.

Loeb, N. G., B. A. Wielicki, D. R. Doelling, G. L. Smith, D. F. Keyes, S. Kato, N. Manalo-Smith, and T. Wong (2009), Toward Optimal Closure of the Earth's Top-of-Atmosphere Radiation Budget, *Journal of Climate*, *22*(3), 748–766, doi:10.1175/2008JCLI2637.1.

Marchand, R. (2013), Trends in ISCCP, MISR, and MODIS cloud-top-height and optical-depth histograms, *Journal of Geophysical Research: Atmospheres*, *118*(4), 1941–1949, doi:10.1002/jgrd.50207.

Marchand, R., T. Ackerman, M. Smyth, and W. B. Rossow (2010), A review of cloud top height and optical depth histograms from MISR, ISCCP, and MODIS, *Journal of Geophysical Research*, *115*(D16), D16,206, doi:10.1029/2009JD013422.

McCoy, D. T., D. L. Hartmann, and D. P. Grosvenor (2014), Observed Southern Ocean Cloud Properties and Shortwave Reflection. Part II: Phase changes and low cloud feedback, *Journal of Climate*, *27*(23), 8858–8868, doi:10.1175/JCLI-D-14-00288.1.

McCoy, D. T., D. L. Hartmann, M. D. Zelinka, P. Ceppi, and D. P. Grosvenor (2015), Mixed-phase cloud physics and Southern Ocean cloud feedback in climate models, *Journal of Geophysical Research: Atmospheres*, *120*, 9539–9554, doi:10.1002/2015JD023603.

O'Dell, C. W., F. J. Wentz, and R. Bennartz (2008), Cloud Liquid Water Path from Satellite-Based Passive Microwave Observations: A New Climatology over the Global Oceans, *Journal of Climate*, *21*(8), 1721–1739, doi:10.1175/2007JCLI1958.1.

Pincus, R., S. Platnick, S. A. Ackerman, R. S. Hemler, and R. J. Patrick Hofmann (2012), Reconciling Simulated and Observed Views of Clouds: MODIS, ISCCP, and the Limits of Instrument Simulators, *Journal of Climate*, *25*(13), 4699–4720, doi:10.1175/JCLI-D-11-00267.1.

Platnick, S., M. King, S. Ackerman, W. Menzel, B. Baum, J. Riedi, and R. Frey (2003), The MODIS cloud products: algorithms and examples from terra, *IEEE Transactions on Geoscience and Remote Sensing*, *41*(2), 459–473, doi:10.1109/TGRS.2002.808301.

Qu, X., A. Hall, S. A. Klein, and A. M. DeAngelis (2015), Positive tropical marine low-cloud cover feedback inferred from cloud-controlling factors, *Geophysical Research Letters*, *42*(18), 7767–7775, doi:10.1002/2015GL065627.

Rossow, W. B., and R. A. Schiffer (1999), Advances in Understanding Clouds from ISCCP, *Bulletin of the American Meteorological Society*, *80*(11), 2261–2287, doi:10.1175/1520-0477(1999)080⟨2261:AIUCFI⟩2.0.CO;2.

Sherwood, S. C., S. Bony, and J.-L. Dufresne (2014), Spread in model climate sensitivity traced to atmospheric convective mixing, *Nature*, *505*(7481), 37–42, doi:10.1038/nature12829.

Sherwood, S. C., S. Bony, O. Boucher, C. Bretherton, P. M. Forster, J. M. Gregory, and B. Stevens (2015), Adjustments in the Forcing-Feedback Framework for Understanding Climate Change, *Bulletin of the American Meteorological Society*, *96*(2), 217–228, doi:10.1175/BAMS-D-13-00167.1.

Somerville, R. C. J., and L. A. Remer (1984), Cloud optical thickness feedbacks in the CO2 climate problem, *Journal of Geophysical Research*, *89*(D6), 9668, doi:10.1029/JD089iD06p09668.

Stephens, G. L. (1978), Radiation Profiles in Extended Water Clouds. II: Parameterization Schemes, *Journal of the Atmospheric Sciences*, *35*(11), 2123–2132, doi:10.1175/1520-0469(1978)035⟨2123:RPIEWC⟩2.0.CO;2.

Storelvmo, T., I. Tan, and A. V. Korolev (2015), Cloud Phase Changes Induced by CO2 Warming–a Powerful yet Poorly Constrained Cloud-Climate Feedback, *Current Climate Change Reports*, *1*(4), 288–296, doi:10.1007/s40641-015-0026-2.

Taylor, K. E., M. Crucifix, P. Braconnot, C. D. Hewitt, C. Doutriaux, A. J. Broccoli, J. F. B. Mitchell, and M. J. Webb (2007), Estimating Shortwave Radiative Forcing and Response in Climate Models, *Journal of Climate*, *20*(11), 2530–2543, doi:10.1175/JCLI4143.1.

Tselioudis, G., W. B. Rossow, and D. Rind (1992), Global Patterns of Cloud Optical Thickness Variation with Temperature, *Journal of Climate*, *5*(12), 1484–1495, doi:10.1175/1520-0442(1992)005⟨1484:GPOCOT⟩2.0.CO;2.

Tsushima, Y., S. Emori, T. Ogura, M. Kimoto, M. J. Webb, K. D. Williams, M. A. Ringer, B. J. Soden, B. Li, and N. Andronova (2006), Importance of the mixed-phase cloud distribution in the control climate for assessing the response of clouds to carbon dioxide increase: a multi-model study, *Climate Dynamics*, *27*(2-3), 113–126, doi:10.1007/s00382-006-0127-7.

Webb, M., C. Senior, S. Bony, and J.-J. Morcrette (2001), Combining ERBE and ISCCP data to assess clouds in the Hadley Centre, ECMWF and LMD atmospheric climate models, *Climate Dynamics*, *17*(12), 905–922, doi:10.1007/s003820100157.

Webb, M. J., A. P. Lock, C. S. Bretherton, S. Bony, J. N. S. Cole, A. Idelkadi, S. M. Kang, T. Koshiro, H. Kawai, T. Ogura, R. Roehrig, Y. Shin, T. Mauritsen, S. C. Sherwood, J. Vial, M. Watanabe, M. D. Woelfle, and M. Zhao (2015), The impact of parametrized convection on cloud feedback., *Philosophical transactions. Series A, Mathematical, physical, and engineering sciences*, *373*(2054), doi:10.1098/rsta.2014.0414.

Wood, R., and C. S. Bretherton (2006), On the Relationship between Stratiform Low Cloud Cover and Lower-Tropospheric Stability, *Journal of Climate*, *19*(24), 6425–6432, doi:10.1175/JCLI3988.1.

Zelinka, M. D., S. A. Klein, and D. L. Hartmann (2012a), Computing and Partitioning Cloud Feedbacks Using Cloud Property Histograms. Part II: Attribution to Changes in Cloud Amount, Altitude, and Optical Depth, *Journal of Climate*, *25*(11), 3736–3754, doi:10.1175/JCLI-D-11-00249.1.

Zelinka, M. D., S. A. Klein, and D. L. Hartmann (2012b), Computing and Partitioning Cloud Feedbacks Using Cloud Property Histograms. Part I: Cloud Radiative Kernels, *Journal of Climate*, *25*(11), 3715–3735, doi:10.1175/JCLI-D-11-00248.1.

Zelinka, M. D., S. A. Klein, K. E. Taylor, T. Andrews, M. J. Webb, J. M. Gregory, and P. M. Forster (2013), Contributions of Different Cloud Types to Feedbacks and Rapid Adjustments in CMIP5, *Journal of Climate*, *26*(14), 5007–5027, doi:10.1175/JCLI-D-12-00555.1.

Zhang, Y., S. Xie, C. Covey, D. D. Lucas, P. Gleckler, S. A. Klein, J. Tannahill, C. Doutriaux, and R. Klein (2012), Regional assessment of the parameter-dependent performance of CAM4 in simulating tropical clouds, *Geophysical Research Letters*, *39*(14), n/a–n/a, doi:10.1029/2012GL052184.

Zhao, M. (2014), An Investigation of the Connections among Convection, Clouds, and Climate Sensitivity in a Global Climate Model, *Journal of Climate*, *27*(5), 1845–1862, doi:10.1175/JCLI-D-13-00145.1.

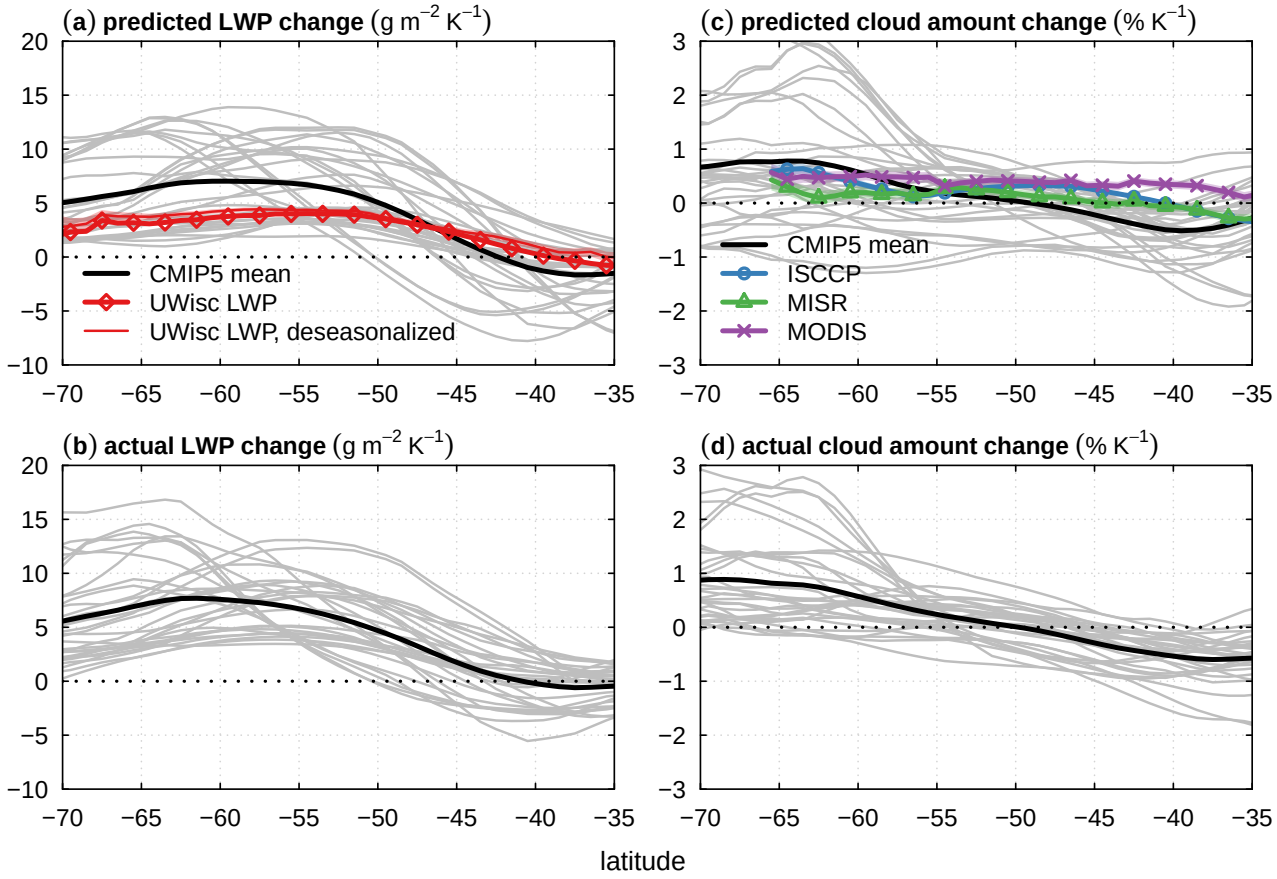

Figure 1. Predicted and actual change in liquid water path (LWP) and cloud amount in CMIP5 models and in observations. The predicted changes (a, c) are based on regressions onto low-level (500–850 hPa) temperature (see Methods); the actual changes (b, d) are calculated as 2081–2100 minus 1981–2000 in the RCP8.5 experiment, normalized by the low-level temperature change in each model. Observed cloud amount is obtained by integrating the cloud property histograms over all cloud top pressure and optical depth bins. Grey curves denote individual models, the thick black curve represents the multi-model mean, and colored curves correspond to observational data sets. For observations, pale color shading denotes the 95% confidence intervals based on a two-sided significance test for the regression slope; these confidence intervals are often not visible due to their narrowness.

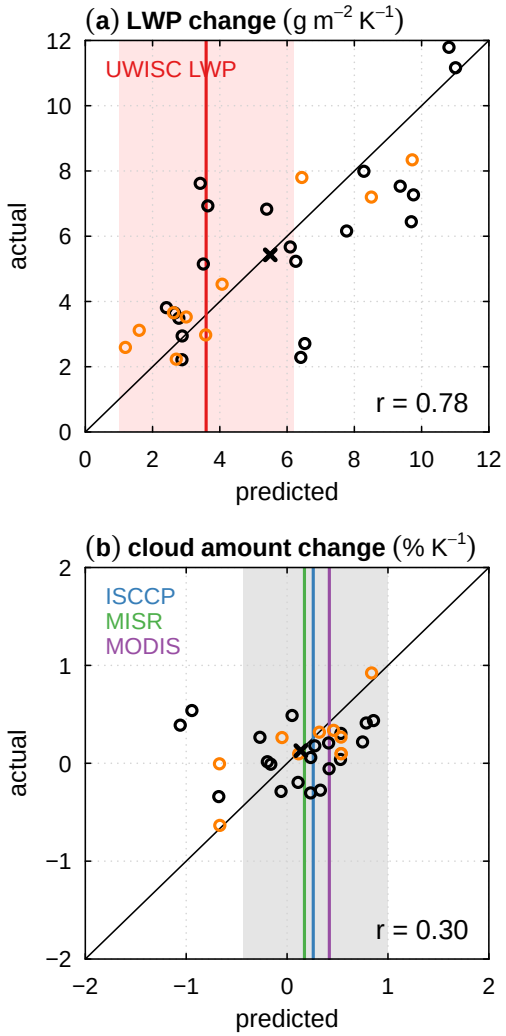

Figure 2. Scatterplots of actual versus predicted (a) LWP change and (b) cloud amount change, both averaged over 45°–60° S. The black crosses mark the multi-model mean. Vertical colored bars denote the predictions associated with observational data sets, and orange open circles indicate the models with cloud property histogram data that were used for the SW cloud feedback calculation in Figs. 4 and 5. Shading represents the 95% uncertainty interval for the mean observational estimates, calculated as described in Text S3.

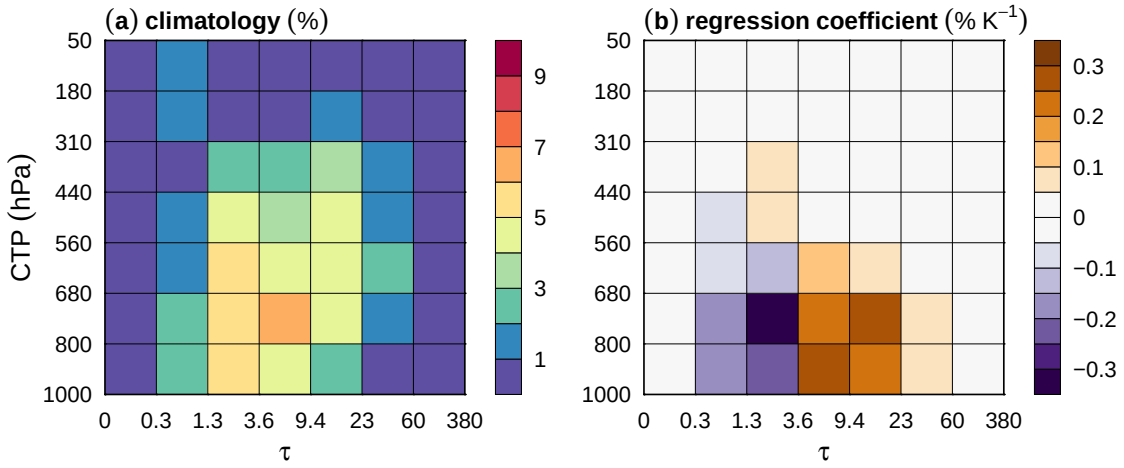

Figure 3. ISCCP cloud fraction histograms binned by cloud top pressure (CTP) and optical depth (τ). The mean climatology is shown in (a) and the regression coefficient on low-level temperature in (b), both averaged over the 45°–60° S latitude range.

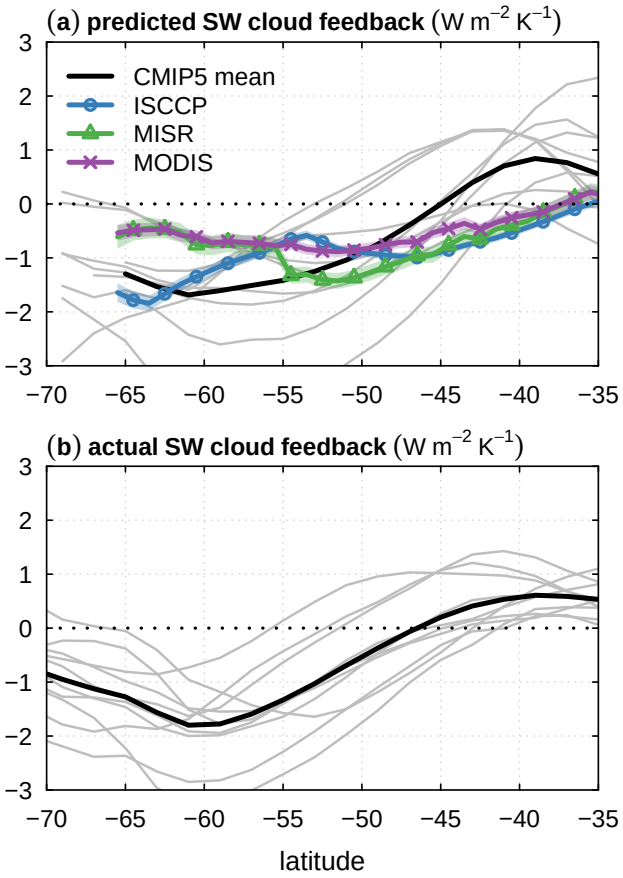

Figure 4. Predicted and actual SW cloud feedback in models and observations. Curves are defined as in Fig. 1. The predicted cloud feedback is obtained by multiplying cloud-radiative kernels [*Zelinka et al.*, 2012b] with cloud fraction histograms regressed on temperature. The actual cloud feedback in (b) is calculated using APRP with RCP8.5 data (see text), and includes cloud adjustments to CO_2 forcing. The feedbacks are normalized by the local low-level temperature change rather than global-mean surface temperature. For observations, pale color shading denotes the 95% confidence intervals based on a two-sided significance test for the regression slope. In panel (a), missing data at high latitudes result from the exclusion of ice- and land-covered grid points from the regression analysis.

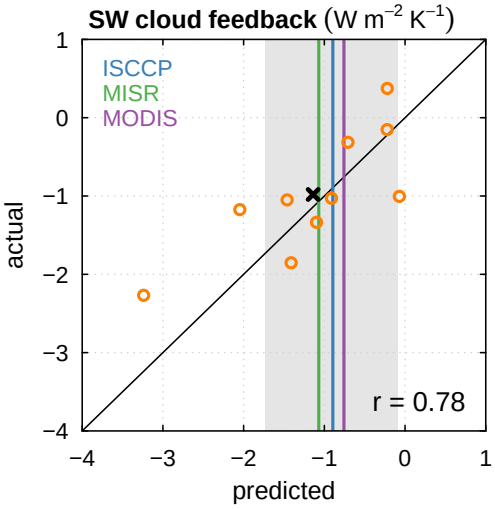

Figure 5. Scatterplot of actual versus predicted SW cloud feedback, averaged over 45°–60° S. Vertical colored bars denote the predictions associated with satellite observations. Grey shading represents the 95% uncertainty interval for the mean of the three observational estimates (Text S3). The black cross marks the multi-model mean. The orange open circles are as in Fig. 2.

Supporting Information for "Observational evidence for a negative shortwave cloud feedback in mid to high latitudes"

Paulo Ceppi,[1,2] Daniel T. McCoy,[1] and Dennis L. Hartmann[1]

Corresponding author: P. Ceppi, Department of Meteorology, University of Reading, Earley Gate, PO Box 243, RG6 6BB, Reading, United Kingdom. (p.ceppi@reading.ac.uk)

[1]Department of Atmospheric Sciences,
University of Washington, Seattle, WA,
USA.

[2]Department of Meteorology, University
of Reading, Reading, United Kingdom.

Contents of this file

1. Text S1 to S3
2. Figures S1 to S4
3. Table S1

Introduction

In addition to four supplementary figures and one table listing the models used in our analysis, in this Supporting Information we provide information on the data sets used in this study (Text S1), discuss some possible sources of error in the satellite retrievals that may affect our results (Text S2), and describe the methodology to calculate observational confidence intervals (Text S3).

Text S1

In this section we provide additional details on the observational products and model data sets used in this study.

The ISCCP, MISR, and MODIS data sets are optimized for comparison with GCM satellite simulators, and are provided in a format identical to standard CMIP5 model output by the Cloud Feedback Model Intercomparison Program (CFMIP; `http://climserv.ipsl.polytechnique.fr/cfmip-obs/`). The ISCCP data are a simulator-oriented version derived from the D1 data set, covering the period July 1983–June 2008 (25 years). For MODIS, Collection 5.1 data are used, covering March 2000–February 2015 (14 years), and including both Terra and Aqua satellite retrievals. Finally, MISR Level 3 data are used, covering June 2000–May 2013 (12 years). Since MISR retrieves cloud top physical height rather than pressure, we interpolate the MISR cloud histograms from height to

pressure coordinates, while conserving total cloud amount. In doing this we assume a simple relationship between pressure p and height z given by $p(z) = p_0 \exp(-z/H)$, with surface pressure $p_0 = 1000$ hPa and scale height $H = 8$ km.

In CMIP5, the most commonly available satellite simulator is the ISCCP simulator (variable clisccp), for which 13 models have provided output in either the historical or AMIP experiments. As in *Zelinka et al.* [2012], we verify correct simulator implementation by comparing the simulator-based total cloud amount (obtained by adding over all cloud top pressure–optical depth bins) with the actual total cloud amount output by each model, and reject models for which the two measures of global-mean climatological cloud amount differ by more than 10 percent. Based on this test, we use cloud histograms from 10 models (crosses in Table S1); the rejected models are IPSL-CM5A-LR, IPSL-CM5A-MR, and MIROC-ESM.

Text S2

In this section we discuss possible sources of error in the satellite retrievals, their possible impact on our results, and our data analysis choices to mitigate such impacts.

ISCCP retrievals suffer from substantial inhomogeneities in time (due to changes in instrumentation) and space (due to the different spatial coverage of geostationary and polar-orbiting satellites) [*Evan et al.*, 2007], and particularly in high latitudes unphysical spatial inhomogeneities in cloud properties are obvious even upon simple visual inspection of the raw data; such spatial artifacts are possibly related to polar-orbiter swaths [*Norris*, 2000]. For this reason, we doubt that the large increase in the negative feedback poleward of 55° S reported by ISCCP is physical (blue curves in Figs. 4a and 6a).

Furthermore, optical depth observations are affected by errors due to temporal variations in viewing and illumination geometry, whose effects depend on instrument technology and retrieval algorithm. Of particular relevance to instruments using solar reflectance such as ISCCP, MODIS, and MISR are the potentially large optical depth biases at the highest solar zenith angles (i.e. at high latitudes during winter), as discussed in section 3 [*Loeb and Davies*, 1996]. For MODIS, these solar zenith angle biases are large and well-documented [*Seethala and Horváth*, 2010; *Grosvenor and Wood*, 2014; *Lebsock and Su*, 2014].

We have attempted to mitigate the impact of such systematic errors by omitting retrievals at solar zenith angles larger than 60° for MODIS and MISR (see Methods). If such values are not excluded from the analysis, the SW cloud feedback predicted by MODIS becomes weaker (less negative) by 0.25 W m^{-2} K^{-1} between 45° and 60° S, but in MISR it strengthens by about 0.67 W m^{-2} K^{-1} (not shown), leading to larger disagreement between observational data sets. Since optical depth is overestimated at the highest solar zenith angles (and therefore at the lowest temperatures, opposing the positive optical depth–temperature relationship), one would expect the illumination angle effect to lead to an underestimation of the negative optical depth feedback, as for the MODIS results. This not being the case for MISR suggests other effects may play a role; for example, complex interactions between viewing and solar zenith angle are known to affect MISR retrievals [*Liang and Di Girolamo*, 2013].

Although we excluded retrievals at the highest illumination angles, it is likely that seasonal variations in solar zenith angle still affect the optical depth–temperature rela-

tionships in our results. Repeating the cloud histogram regressions with deseasonalized data — and thus completely filtering out the possible signal due to solar angle variations — we still obtain increases in cloud optical depth and a negative SW feedback, but the results are very noisy and the historical relationships are poor predictors of the forced response in models (not shown). However, since the observed LWP–temperature relationships remain nearly identical when the seasonal cycle is removed (Fig. 1a), we are confident that the cloud optical depth increase with warming is not an artifact of seasonally-dependent satellite retrieval biases.

While the lower LWP sensitivity to temperature in observations compared to the multi-model mean would suggest that the optical depth feedback is much too negative in models (cf. Fig. 1a), the LWP observations are not exempt from errors either. *Lebsock and Su* [2014] have shown that on average, microwave LWP retrievals (similar to the data set used in this study) tend to substantially overestimate the true LWP, with errors mainly stemming from ambiguities in the detection of cloudy pixels and in the partitioning between cloud and precipitating water. In light of these biases, *Lebsock and Su* [2014] concluded that observational LWP climatologies remain too uncertain to effectively constrain climate model behavior. Thus, we caution that the observed LWP–temperature relationship shown here should not be interpreted in a strictly quantitative sense.

Text S3

Observational confidence intervals are derived from the uncertainty in the prediction of the models' responses based on historical regressions on local temperature. The uncertainty in the prediction of cloud property responses is thus taken as proportional to the

standard deviation of the residuals relative to the one-to-one line in Figs. 2 and 5. Assuming that the residuals are normally distributed, the half-width of the 95% confidence interval is then simply equal to 1.96 times the standard deviation of the residuals. The confidence intervals are calculated relative to the mean observational estimate in Figs. 2b and 5.

Our calculation is similar in concept to the estimation of prediction intervals in linear regression [see e.g. *Wilks*, 2006, Eq. 6.22], but we do not include the terms related to the uncertainty in the intercept and slope of the relationship, since the expected relationship between predicted and actual responses is known (the one-to-one line). Furthermore, here the residuals are calculated as orthogonal departures from the one-to-one line, rather than as vertical departures as in least-squares regression.

The confidence intervals calculated in this manner do not include the uncertainty in the estimation of the observational regression slopes, which is very small in our analysis owing to the robustness of the relationships. More importantly, our calculation also excludes the uncertainty associated with errors in the satellite retrievals, reflected in the differences between the various observational estimates. We believe this uncertainty is mitigated, but not fully suppressed, by taking the mean of the three observational estimates as the most likely observational value.

References

Evan, A. T., A. K. Heidinger, and D. J. Vimont (2007), Arguments against a physical long-term trend in global ISCCP cloud amounts, *Geophysical Research Letters*, *34*(4), L04,701, doi:10.1029/2006GL028083.

Grosvenor, D. P., and R. Wood (2014), The effect of solar zenith angle on MODIS cloud optical and microphysical retrievals within marine liquid water clouds, *Atmospheric Chemistry and Physics*, *14*(14), 7291–7321, doi:10.5194/acp-14-7291-2014.

Lebsock, M., and H. Su (2014), Application of active spaceborne remote sensing for understanding biases between passive cloud water path retrievals, *Journal of Geophysical Research: Atmospheres*, *119*(14), 8962–8979, doi:10.1002/2014JD021568.

Liang, L., and L. Di Girolamo (2013), A global analysis on the view-angle dependence of plane-parallel oceanic liquid water cloud optical thickness using data synergy from MISR and MODIS, *Journal of Geophysical Research: Atmospheres*, *118*(5), 2389–2403, doi:10.1029/2012JD018201.

Loeb, N. G., and R. Davies (1996), Observational evidence of plane parallel model biases: Apparent dependence of cloud optical depth on solar zenith angle, *Journal of Geophysical Research*, *101*(D1), 1621, doi:10.1029/95JD03298.

Norris, J. R. (2000), What Can Cloud Observations Tell Us About Climate Variability?, *Space Science Reviews*, *94*(1), 375–380, doi:10.1023/A:1026704314326.

Seethala, C., and Á. Horváth (2010), Global assessment of AMSR-E and MODIS cloud liquid water path retrievals in warm oceanic clouds, *Journal of Geophysical Research*, *115*(D13), D13,202, doi:10.1029/2009JD012662.

Wilks, D. S. (2006), *Statistical Methods in the Atmospheric Sciences*, 648 pp., Academic Press.

Zelinka, M. D., S. A. Klein, and D. L. Hartmann (2012), Computing and Partitioning Cloud Feedbacks Using Cloud Property Histograms. Part I: Cloud Radiative Kernels,

Journal of Climate, *25*(11), 3715–3735, doi:10.1175/JCLI-D-11-00248.1.

Zelinka, M. D., S. A. Klein, K. E. Taylor, T. Andrews, M. J. Webb, J. M. Gregory, and P. M. Forster (2013), Contributions of Different Cloud Types to Feedbacks and Rapid Adjustments in CMIP5, *Journal of Climate*, *26*(14), 5007–5027, doi:10.1175/JCLI-D-12-00555.1.

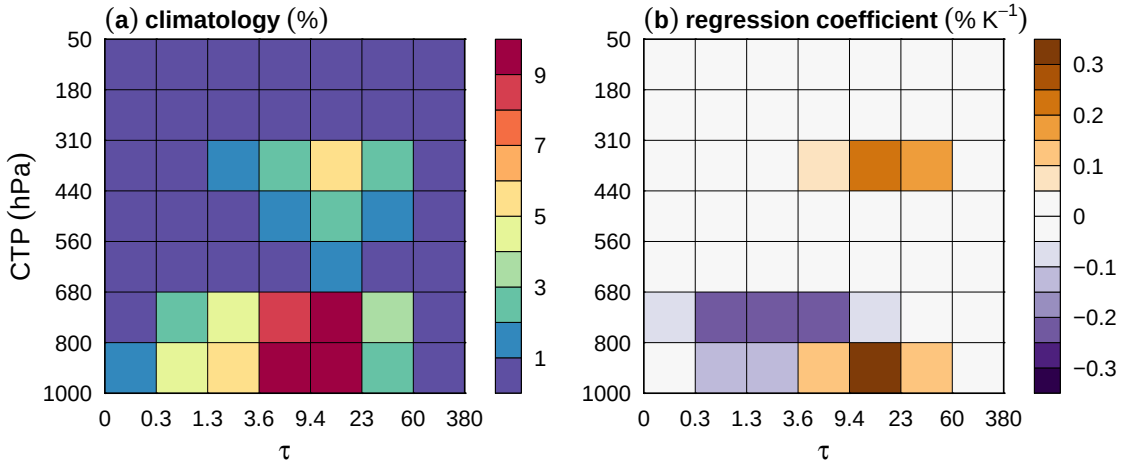

Figure S1. As in Fig. 3, but for MISR. The cloud amount values have been remapped from cloud top height bins to cloud top pressure bins (see Text S1) for consistency with the cloud-radiative kernels.

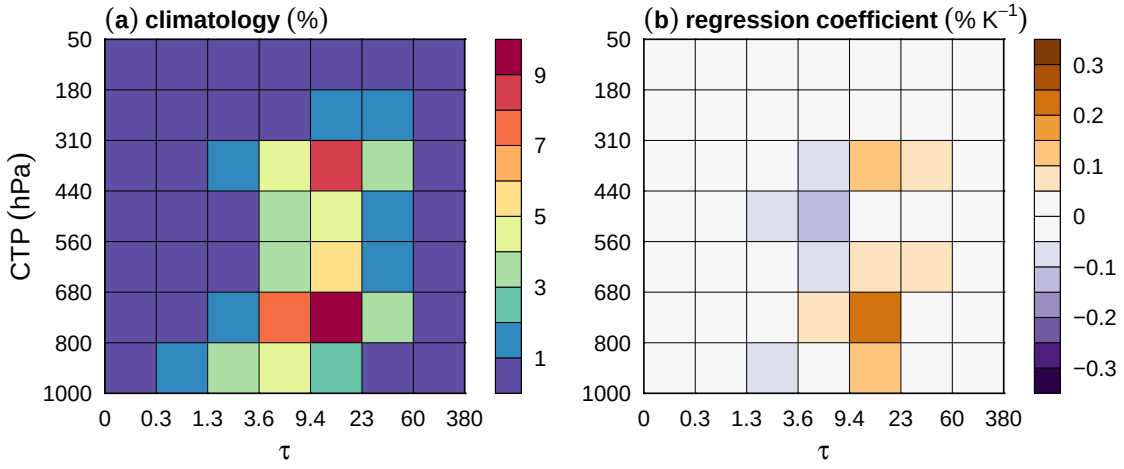

Figure S2. As in Fig. 3, but for MODIS.

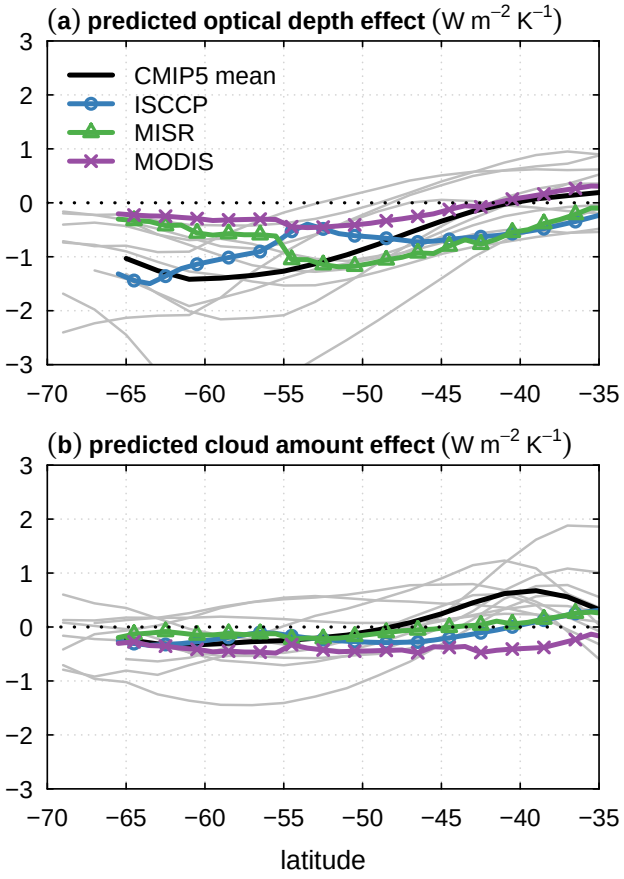

Figure S3. As in Fig. 4, but partitioning the cloud feedback into effects of (a) optical depth changes and (b) cloud amount changes, following *Zelinka et al.* [2013]. Confidence intervals are omitted.

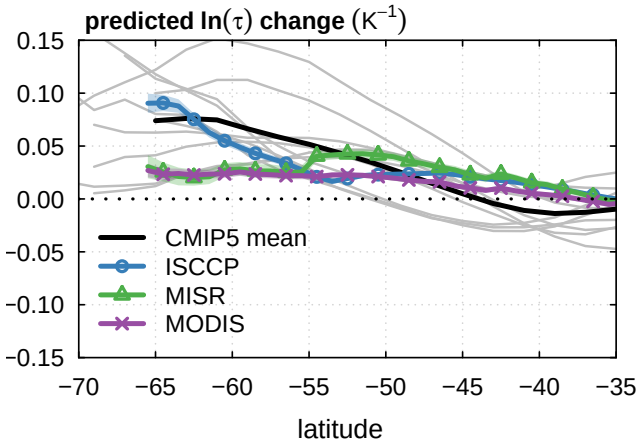

Figure S4. Predicted change in the natural logarithm of optical depth, $\ln(\tau)$, calculated by regressing $\ln(\tau)$ onto low-level temperature. Here optical depth is simply calculated as the weighted mean of the 7 optical depth bins in the cloud property histograms, using the total cloud amount values in each bin as weights.

Table S1. List of CMIP5 models used in our analyses. A cross (×) indicates the models that provided historical or AMIP cloud property histograms using an ISCCP simulator. All 30 models listed below provided LWP, total cloud amount, as well as temperature data for the historical and RCP8.5 experiments. For each model, only the first ensemble member is used.

	Model name	historical	AMIP
1	ACCESS1.0		
2	ACCESS1.3		
3	BCC-CSM1.1		
4	BCC-CSM1.1(m)		×
5	CanESM2	×	
6	CCSM4		×
7	CESM1-BGC		
8	CESM1-CAM5		×
9	CNRM-CM5		×
10	CSIRO-Mk3.6.0		
11	FIO-ESM		
12	GFDL-CM3		×
13	GFDL-ESM2G		
14	GFDL-ESM2M		
15	GISS-E2-H		
16	GISS-E2-R		
17	HadGEM2-CC		
18	HadGEM2-ES	×	
19	INMCM4		
20	IPSL-CM5A-LR		
21	IPSL-CM5B-LR		
22	IPSL-CM5A-MR		
23	MIROC5	×	
24	MIROC-ESM		
25	MIROC-ESM-CHEM		
26	MPI-ESM-LR	×	
27	MPI-ESM-MR		
28	MRI-CGCM3	×	
29	NorESM1-M		
30	NorESM1-ME		